

# A Low-Cost IoT System for Indoor Positioning Targeting Assistive Environments

Vasileios Serasidis  
*Department of Physics*  
*Aristotle University of Thessaloniki*  
Thessaloniki, Greece

Ioannis Sofianidis  
*Department of Physics*  
*Aristotle University of Thessaloniki*  
Thessaloniki, Greece

George Margaritis  
*Department of Physics*  
*Aristotle University of Thessaloniki*  
Thessaloniki, Greece

Christos Sad  
*Department of Physics*  
*Aristotle University of Thessaloniki*  
Thessaloniki, Greece

Vasileios Konstantakos  
*Department of Physics*  
*Aristotle University of Thessaloniki*  
Thessaloniki, Greece

Kostas Siozios  
*Department of Physics*  
*Aristotle University of Thessaloniki*  
Thessaloniki, Greece

**Abstract**—The elderly population is increasing, imposing among others a continues demand for customized health-care solutions. Many of these systems rely on accurate indoor positioning in order to activate actuators’ functionalities at assisted environments. Typically these systems rely to Bluetooth and WiFi beacons with accuracy around 1 meter. Throughout this paper, we introduce a low-cost embedded system that rely on Ultra-WideBand technology to enable accurate indoor positioning and navigation. Experimental results with different scenarios highlight the superiority of proposed platform, since the mean error between estimated and actual path can be up to 5-7cm.

**Index Terms**—Indoor positioning, IoT, Low-cost, Beacon technology

## I. INTRODUCTION

With an ever-growing elderly population, various ambient assisted living (AAL) technologies have been proposed. These systems rely on embedded, and Internet-of-Things (IoT) systems, to enable independent living and improve the quality of life of elder people. Since the majority of these systems are triggered based on people movement and/or their location within houses, these systems rely on technologies for indoor positioning. Moreover, recent studies indicated that the monitor and study behavioral patterns is a useful tool for early detection of some degenerative diseases, such as Alzheimer’s disease [1] [2] [3] [4].

During the last decade many indoor positioning systems have been presented, most of them relying on fingerprinting-based and proximity technologies. In detail, there are solutions for indoor positioning that rely on WiFi [5] and Bluetooth [6] beacons that rely on fingerprint. More specifically, the fingerprint refers to an RSSI (Received Signal Strength Indicator) feature vector composed of received signal values from different emitting devices or beacons. In case we also consider the position of beacon deployment, the previously mentioned technologies can also support proximity-based functionality. GPS-based solutions [7] can also be used for this purpose, but

with limited applicability due to attenuation of the satellite signal to indoor environments.

The previously mentioned systems support indoor positioning in room-scale size to activate a device when somebody enters/leaves to/from a room. The majority of these solutions rely on sensors that trigger events to enable more advanced functionalities and services, such as to control lighting, windows, doors, locks, water outlets, etc. However, the limited accuracy of estimations cannot support more advanced services related to the positioning or navigation of elderly people within the room. To overcome this drawback, algorithms that improve accuracy were also explored [6] [5]. However, these algorithms have increased computational complexity; thus, their execution cannot be performed onto low-cost embedded devices.

Throughout this paper, we introduce an indoor positioning system to monitor the behavior of older persons, which in turn can be used as a valuable tool for multiple assisted living services. The proposed solution relies on a Ultra-WideBand (UWB) technology, which enables higher precision measurements. Experimental results with different operating configuration scenarios and trajectories highlight the superiority of introduced solution, as we achieve average accuracy in indoor positioning ranging between 5–7cm. Additionally, the reduced computational complexity of proposed system is also crucial, since it can be implemented as part of a low-cost embedded device with limited maintenance cost (e.g. power charges). Finally, the proposed solution is easily expandable with the minimum engineering cost. Since each room has its own accuracy constraints (e.g. based on furniture), accurate indoor positioning will require different number of anchors.

The rest of the paper is organized, as follows: Section II describes the proposed architecture for the indoor positioning solution. The algorithmic approach for this system is discussed in Section III. Experimental results that highlight the efficiency of the proposed solution as compared to state-of-the-art relevant products are provided at Section IV. Finally, Section V concludes the paper.

## II. ARCHITECTURE OF PROPOSED LOCALIZATION SYSTEM

This section describes the architecture of the proposed low-cost IoT system for indoor positioning and navigation. Figure 1 gives an overview of this architecture consisted of three types of components, namely the anchors, the tags and the local hub. The system's installation phase impose to assign anchors to predefined locations ( $x$  and  $y$  coordinates in home scale), while tag(s) can be randomly moved within this area. In order to maximize the accuracy, anchors location should be carefully selected to support sufficient area coverage. Based on our exploration, we conclude that 4 – 6 anchors should be placed per room. These anchors should be uniformly distributed over the room's area by taking into consideration the phenomena of reflection, refraction, diffraction, absorption, and scattering (e.g. from dark points) [9].

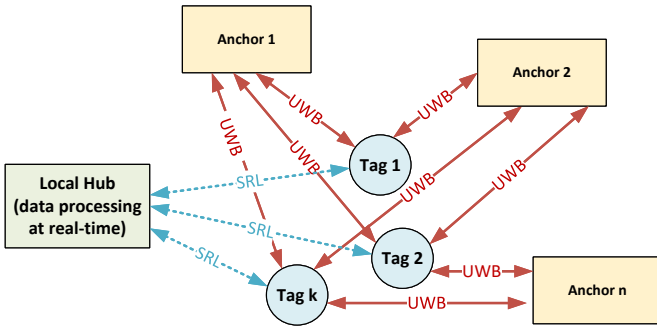


Fig. 1: Architecture of the proposed indoor positioning system.

### A. Calculate Time-of-Flight

In order to enable each tag to calculate its own distance from any anchor, our solution relies on time-of-flight metric. In relevant literature there are alternative approaches dealing with this topic, each of which exhibits advantages and disadvantages. Among others, widely adopted solutions include *time of arrival* (ToA) and *time-difference of arrival* (TDoA) techniques. More precisely, the ToA technique measures the time elapsed from message transmission (source node) until it is received (target node). This technique pre-require that the devices clocks must be synchronized, which is extremely difficult especially when we deal with low-cost solutions (even a negligible offset in clocks might result to hundreds of meters accuracy loss). A similar approach is TDoA, where the tag receives a message that is periodically transmitted from each anchor. Since the functionality of this technique relies on calculating the time difference between message receipt at system's receiver nodes, these receivers must be synchronized. Thus, this approach has also limited applicability to low-cost indoor positioning systems.

The proposed indoor positioning system relies on Two-Way-Ranging (TWR) technique, which is schematically depicted at Figure 2. Since this approach does not distinguish between transmitter and receiver node, both tag and anchors transmit and receive messages. Without affecting the general applicability of this approach, we will assume that the tag (moving

person) initiates periodically a task for positioning estimation. For this purpose, it broadcasts a packet that contains tag's unique ID ( $tag\_id$ ) and timestamp  $t_1$  (refers to the time of transmission). In case an anchor receives such a packet, it replies by attaching its own unique ID ( $anchor\_id$ ), the time of packet's receipt (timestamp  $t_2$ ), as well as the time of new transmission (timestamp  $t_3$ ). Finally, if a tag receives anchor's transmission, it checks whether its own id ( $tag\_id$ ) can be found inside the packet. If yes, it attaches the current timestamp ( $t_4$ ) and the packet is further processed in order to calculate the time-of-flight (ToF) based on Equation 1. Note that the ToF metric is proportional to the distance (in meters) between tag and anchor.

$$ToF = \frac{(t_4 - t_1) - (t_3 - t_2)}{2} \quad (1)$$

Since the TWR technique does not require any kind of clock synchronization, it exhibits higher flexibility and applicability, as compared to the ToA and TDoA techniques discussed previously. However, the main drawback of this technique affects the more message transmission to calculate time difference, which in turn might affect the mobile nodes' energy autonomy. In order to overcome this challenge, next subsection explores also the impact of network transmission protocol.

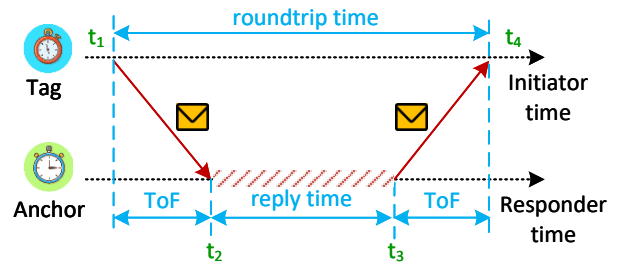


Fig. 2: Distance calculation between tag and anchor.

## III. INDOOR POSITIONING

Having as input the distances from tag to room's tags (as they are were computed based on ToF metric with Equation 1), this section describes the calculation of tag's ( $x$ ,  $y$ ) location within a room. Our system applies the trilateration method, which calculates the Cartesian coordinates of tag based at least on 3 reference points (anchors). For demonstration purposes, lets assume that our architecture consists of 1 tag and 3 anchors (marked with A, B and C), as it is depicted at Figure 3. In such a case, the radius of each circle (Euclidean distance) is computed according to Equations 2–4.

$$r1 = \sqrt{(x - x_1)^2 + (y - y_1)^2} \quad (2)$$

$$r2 = \sqrt{(x - x_2)^2 + (y - y_2)^2} \quad (3)$$

$$r3 = \sqrt{(x - x_3)^2 + (y - y_3)^2} \quad (4)$$

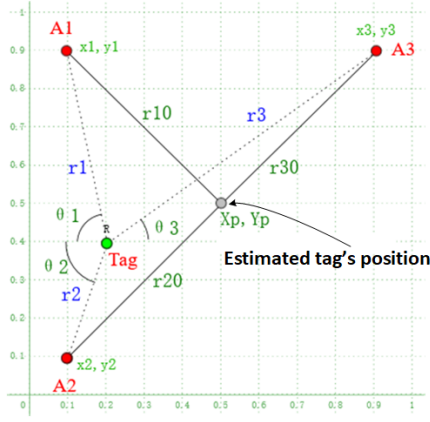


Fig. 3: Positioning estimation based on trilateration method.

In order to solve these equations, we apply the least squares error method, which exhibits limited computational complexity and can be deployed in low-performance embedded devices. More specifically, the previously mentioned equations can be represented in the following form:

$$(x - x_1)^2 + (y - y_1)^2 - [(x - x_2)^2 + (y - y_2)^2] = r_1^2 - r_2^2 \quad (5)$$

$$(x - x_1)^2 + (y - y_1)^2 - [(x - x_3)^2 + (y - y_3)^2] = r_1^2 - r_3^2 \quad (6)$$

Hence, the Equations 5 and 6 can be represented in the form of tables  $Ax = b$ , as it is depicted at Equation 7. The solution of this equation is retrieved according to  $X = A^{-1}b$ . In case, the system has more anchors ( $A_1, A_2, \dots, A_x$ ) than tags, the tag's position is calculated based on  $X = (A^T A)^{-1} A^T b$ .

$$2 \underbrace{\begin{pmatrix} x_2 - x_1 & y_2 - y_1 \\ x_3 - x_1 & y_3 - y_1 \end{pmatrix}}_A \times \underbrace{\begin{pmatrix} x \\ y \end{pmatrix}}_X = \underbrace{\begin{pmatrix} r_1^2 - r_2^2 - x_1^2 - y_1^2 + x_2^2 + y_2^2 \\ r_1^2 - r_3^2 - x_1^2 - y_1^2 + x_3^2 + y_3^2 \end{pmatrix}}_b \quad (7)$$

The accuracy of tag's positioning can be further improved with the iterative least squares (RLS) method. In detail, RLS is an adaptive filter algorithm that iteratively finds the coefficients that minimize a weighted linear least squares cost function relating to the input signals.

In order to implement this method, initially we assume that tag's location is  $(X_p, Y_p)$ , where the distance from all the anchors is the same (as it is depicted at Figure 3). Next, we summarize the sine and cosine for angles  $\theta_1, \theta_2$ , and  $\theta_3$ . Also, we calculate the difference between radius  $r_1 - r_{10}$ ,  $r_2 - r_{20}$ , and  $r_3 - r_{30}$  found in table  $b$ . These data are fed to the least square algorithm in order to calculate the anchor's deviation versus its previous positioning  $(X_p, Y_p)$ . Finally, we refine tag's position and repeat iteratively algorithm until the error to be minimized (the values of array  $b$  to be minimized). For demonstration purposes, the previously mentioned analysis refers to a case with 3 anchors and 1 tag; however, it is also applicable to any other system configuration.

The pseudocode depicted at Algorithm 1 implements the functionality of calculating tag's position with the proposed framework.

---

**Algorithm 1** Proposed algorithm for indoor positioning.

---

**Require:**  $max\_iterations \geq 0$   
0: **while**  $i \neq max\_iterations$  **do**  
0:  $r_{10} \leftarrow \sqrt{(X_p - X_1)^2 + (Y_p - Y_1)^2}$   
0:  $r_{20} \leftarrow \sqrt{(X_p - X_2)^2 + (Y_p - Y_2)^2}$   
0:  $r_{30} \leftarrow \sqrt{(X_p - X_3)^2 + (Y_p - Y_3)^2}$   
0:  $A \leftarrow \left[ \frac{X_p - X_1}{r_1} * \frac{Y_p - Y_1}{r_1}; \frac{X_p - X_2}{r_2} * \frac{Y_p - Y_2}{r_2}; \frac{X_p - X_3}{r_3} * \frac{Y_p - Y_3}{r_3} \right]$   
0:  $b \leftarrow [r_1 - r_{10}; r_2 - r_{20}; r_3 - r_{30}]$   
0:  $X \leftarrow \frac{1}{(A^T * A)} * (A^T * b)$   
0:  $X_p \leftarrow X_p + X(1)$   
0:  $X_p \leftarrow X_p + X(2)$   
0: **if** ( $b$  improvement is negligible) **then**  
0:     stop iterations  
0: **end if**  
0: **end while** = 0

---

In order to further improve the accuracy of our system, we apply a complementary filter, which consists of a combination of a Low-Pass Filter (LPF) and a High-Pass Filter (HPF). Such a min-max approach reduces signal noise towards improving the accuracy of localization estimations. The efficiency of this filter depends on the  $a$  parameter (in the range of  $[0, 1]$ ), which defines that the algorithm will compute current output based on  $(1 - a)\%$  of the previous value increased by  $a\%$  of the current value. Previous studies indicate that complementary filter outperforms Kalman filter significantly by using less computational and processing power and providing more accuracy [8].

#### IV. EXPERIMENTAL RESULTS

The proposed indoor positioning system was implemented based on DWM1001-DEV development board that rely on UWB technology [10]. For evaluation purposes, the system consisted of 6 anchors and 1 tag was applied to a large-scale room depicted at Figures 5(a) and 5(b). The data transfer between each tag and the available anchors is performed based on the architecture depicted at Figure 4. Without affecting the general applicability of the proposed solution, for evaluation purposes, the data processing is performed online to an external PC. However, in the near future we plan to perform this functionality within tag (at a Raspberry Pi processing node). The efficiency of the proposed solution was evaluated with three representative scenarios (i.e. movements) within a room, namely a diagonal (Figure 6), a zig-zag (Figure 7) and a random path (Figure 8).

##### A. Diagonal Path

The efficiency of the proposed indoor positioning system was initially evaluated based on a diagonal path. The results to this analysis (output of trilateration method) regarding both the raw data and the proposed positioning framework

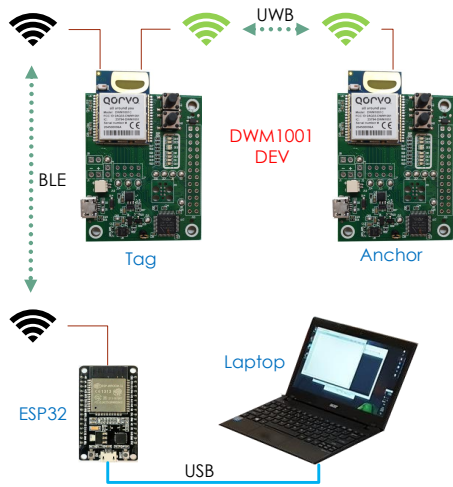


Fig. 4: Architecture of the Tag-Anchor data transfer.



Fig. 5: Anchors placement within the room: (a) A2, A3, A4, A5, (b) A1, A5, A6.

(based on iterative mean square error and complementary filter) are depicted at Figure 6 with red- and purple-colored lines, respectively. At this figure we depict also with green color line the reference solution (ground-truth path).

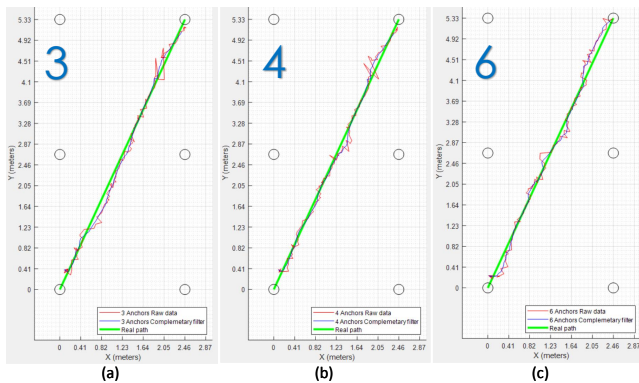


Fig. 6: Accuracy of proposed indoor positioning system with 3, 4, and 6 anchors vs. ground-truth data for diagonal path.

The diagonal path is the simplest one among the studied movements and it is used in order to quantify the efficiency perform computations based on different number of available anchors. In detail, we explore the accuracy to determine

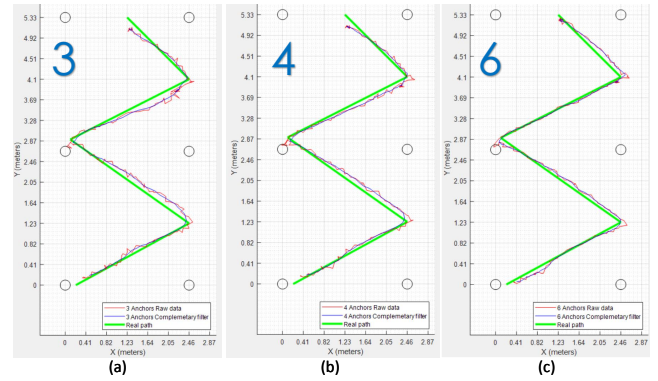


Fig. 7: Accuracy of proposed indoor positioning system with 3, 4, and 6 anchors vs. ground-truth data for zig-zag path.

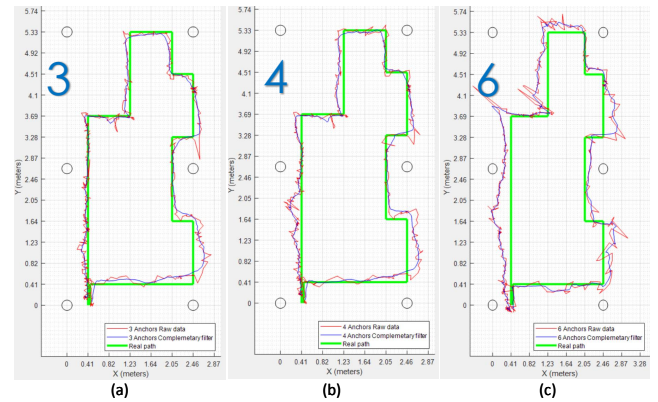


Fig. 8: Accuracy of proposed indoor positioning system with 3, 4, and 6 anchors vs. ground-truth data for random path.

tag's position when the proposed algorithms consider signal measurements from 3, 4 and 5 anchors. For this purpose, computations are performed based only on the 3 and 4 closest anchors to the tag (based on the time-of-flight metric). The results from this analysis are summarized at Table II. According to this analysis, the proposed system results to accuracy errors ranging from 3–4.8cm, on average.

### B. Zig-Zag Path

A zig-zag pattern quantifies system's response for frequent changes to the tag direction. The results to this analysis (output of trilateration method) regarding both the raw data and the proposed positioning framework (based on iterative mean square error and complementary filter, depicted with red- and purple-colored lines respectively, can be found at Figure 7. The reference to this analysis is the ground-truth path depicted with green color line.

For shake of completeness, we also explore the same scenario when position is calculated with fewer anchors. For this purpose, computations are performed only the 3 and 4 closest anchors to the tag (based on the time-of-flight metric). The results from this analysis are summarized at Table II.

Based on this analysis, we conclude that the proposed system achieves superior performance for all the studied

TABLE I: Statistical analysis regarding the diagonal path (error based on ground-truth) in cm.

	Raw	Proposed	Raw	Proposed	Raw	Proposed
Num. Anchors	3	3	4	4	6	6
Min	0.119	0.051	0.038	0.026	0.014	0.013
Max	20.34	11.23	26.36	11.06	19.75	13.16
Mean	5.563	4.224	4.775	3.084	5.661	4.843
Median	5.052	4.261	3.839	2.222	4.106	4.579
Standard deviation	4.128	2.954	4.442	2.767	4.863	3.529

TABLE II: Statistical analysis regarding the zig-zag path (error based on ground-truth) in cm.

	Raw	Proposed	Raw	Proposed	Raw	Proposed
Num. Anchors	3	3	4	4	6	6
Min	0.019	0.013	0.084	0.083	0.035	0.024
Max	26.66	16.89	22.10	14.31	22.06	15.21
Mean	7.746	7.371	7.315	6.848	4.678	3.965
Median	7.608	7.381	7.170	7.484	3.407	3.230
Standard deviation	5.081	4.353	4.171	3.760	4.200	3.390

TABLE III: Statistical analysis regarding the random path (error based on ground-truth) in cm.

	Raw	Proposed	Raw	Proposed	Raw	Proposed
Num. Anchors	3	3	4	4	6	6
Min	7.381	0.555	0.0161	0.059	0.023	0.015
Max	35.42	26.80	34.50	25.04	85.17	44.61
Mean	5.832	5.640	7.268	7.072	14.48	13.80
Median	4.367	4.601	5.333	5.350	13.01	13.24
Standard deviation	5.310	4.763	6.448	5.422	11.13	9.547

configuration setups. Specifically, we reported to improve both minimum and maximum error for the whole path, which range from 0.013cm up to 15cm. Also, standard deviation metric for this path also confirms this superiority, as the values range from 4.3cm (regarding 3 anchors) up to 3.39cm (for 6 anchors).

### C. Random Path

Next, we evaluate also a more complex path, where tag is moved across the whole room, as it is depicted at Figure 8. This figure visualizes the results of this analysis regarding the raw data and the proposed algorithm, as compared to the ground-truth data. This scenario aims to stress the indoor positioning algorithm with additional turns, as well as movements across different directions. In order to further quantify this analysis, Table III provides the statistical analysis of algorithm's accuracy regarding system configurations with 3, 4 and 6 anchors. Similar to previous analysis for the zig-zag movement, the minimum and maximum error for the proposed indoor positioning system range between 0.015cm and 26cm, respectively. Regarding the mean error, it ranges from 5cm (when only the 3 closest anchors are considered) up to 13cm (for the scenario with 6 anchors).

## V. CONCLUSIONS

A novel system for indoor positioning, was introduced. The proposed solution relies on a low-cost UWB beacon technology in order to calculate accurately the distance between movement tag and the anchors. Experimental results highlighted the superiority of introduced solution, as the mean error between estimated and actual path can be up to 5-7cm for the two representative paths studied throughout this paper.

## ACKNOWLEDGMENT

This research has been co-financed by the European Regional Development Fund of the European Union and Greek national funds through the Operational Program Competitiveness, Entrepreneurship and Innovation, under the call RESEARCH – CREATE – INNOVATE (project code: T2EDK-02564).

## REFERENCES

- [1] B. Lyons, et al., "Pervasive Computing Technologies to Continuously Assess Alzheimer's Disease Progression and Intervention Efficacy", *Frontiers in aging neuroscience*, vol. 7, No. 102, June 2015.
- [2] P. Barsocchi, et.al., "Monitoring elderly behavior via indoor position-based stigmergy", *Pervasive and Mobile Computing*, Vol. 23, pp. 26–42, 2015.
- [3] P. Dawadi, D. Cook, M. Schmitter-Edgecombe, "Automated Cognitive Health Assessment From Smart Home-Based Behavior Data", *IEEE J. Biomed. Health Inform.* Vol. 20, pp. 1188-1194, 2015.
- [4] A. Alberdi, et.al., "Automatic assessment of functional health decline in older adults based on smart home data", *Journal of Biomedical Informatics*, Vol. 81, pp. 119-130, 2018.
- [5] X. Du, et.al., "MapSense: Mitigating Inconsistent WiFi Signals Using Signal Patterns and Pathway Map for Indoor Positioning," *IEEE Internet of Things Journal*, vol. 5, no. 6, pp. 4652-4662, Dec. 2018.
- [6] L. Bai, F. Ciravegna, R. Bond and M. Mulvenna, "A Low Cost Indoor Positioning System Using Bluetooth Low Energy," in *IEEE Access*, vol. 8, pp. 136858-136871, 2020.
- [7] X. Li, "A GPS-Based Indoor Positioning System With Delayed Repeaters," in *IEEE Trans. on Vehicular Technology*, vol. 68, no. 2, pp. 1688-1701, Feb. 2019.
- [8] Xiaolin Liang, et.al., "Improved denoising method for through-wall vital sign detection using UWB impulse radar", *Digital Signal Processing*, Vol. 74, pp 72-93, 2018.
- [9] Zou Y, Liu H. TDOA localization with unknown signal propagation speed and sensor position errors. *IEEE Communications Letters*. 2020 Jan 21;24(5):1024-7.
- [10] Qorvo DWM1001-DEV Module Development Board, available online <https://www.decawave.com/product/dwm1001-development-board/>